LANGMUIR Article
Cite This: Langmuir 2019, 35, 6870−6877
pubs.acs.org/Langmuir

Theoretical and Experimental Study of Reversible and Stable Wetting States of a Hierarchically Wrinkled Surface Tuned by Mechanical Strain

Huaping Wu,*,† Sihang Yu,† Zhenxiong Xu,† Binbin Cao,† Xiang Peng,† Zheng Zhang,† Guozhong Chai,*,† and Aiping Liu‡

†Key Laboratory of E&M, Ministry of Education & Zhejiang Province, Zhejiang University of Technology, Hangzhou 310014, China

‡Center for Optoelectronics Materials and Devices, Zhejiang Sci-Tech University, Hangzhou 310018, China

Supporting Information

ABSTRACT: The wetting behavior of hierarchically wrinkled surfaces has attracted great interest because of its broad application in flexible electronic, microfluidic chip, and biomedicine. However, theoretical studies concerning the relationship between the apparent contact angle and mechanical strain applied on the soft and flexible surface with a hierarchically wrinkled structure are still limited. We established a theoretical framework to describe and understand how prestrain and applied dynamic strain reversibly tune the wettability of the hierarchically wrinkled surface. More specifically, a direct relationship between the mechanical strain and contact angle was built through reversible tuning of the amplitude and the wavelength of the wrinkled structures caused by mechanical strain, which allowed for more precise adjustment of surface wettability. To verify the accuracy of the theoretical relationship between the contact angle and mechanical strain, a soft surface with a hierarchically wrinkled structure was prepared by combining wrinkled microstructures and strip ones. The results showed that the experimental contact angles were in agreement with the theoretical ones within a limited error range. This will be helpful for further investigation on the wettability of hierarchically wrinkled surfaces.

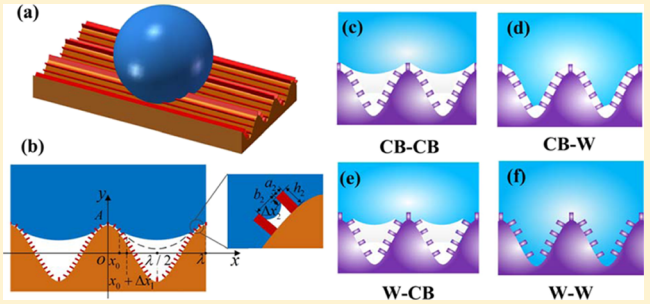

INTRODUCTION

Wettability is one of the basic characteristics of a surface. The self-cleaning ability of the surface, removal of droplets, cell adhesion, and oil−water separation are all closely related to surface wettability.[1−7] Researchers find that the wettability of various surfaces is related to the surface energy and surface roughness, and the hierarchical structures with low surface energy and significant roughness make the surface superhydrophobic.[8−11] Research concerning the surface wettability of hierarchical structures of rigid materials is very thorough.[12−18] Compared with rigid materials, soft materials are more widely used in microfluidic chips,[19−22] soft robots,[23] wearable devices,[24−27] and so forth. However, studies concerning the surface wettability of soft materials have not been widely reported and further exploration is required.

Among the structures used to study the wettability of soft materials, wrinkled structures are the most common.[28−31] With regard to theoretical research concerning wrinkled surfaces, Liu et al. approximated a sine wave structure to study the relationship between the wrinkled size and surface wettability.[32] This theory was further extended to the analysis of the influence of different structures on wettability.[33] Zhang et al. employed the theories of structural wrinkling and solid−liquid contact to design a hierarchically wrinkled surface which could be mechanically tuned between superhydrophilic and superhydrophobic by an applied strain.[34] However, they did not provide a wetting state diagram of hierarchically wrinkled surfaces nor did theoretically predict the relationship between the surface contact angle and applied strain to hierarchically wrinkled surfaces. In terms of experimental research, the hierarchical structures on the wrinkled soft surface are usually varied and prepared by using lithography, laser etching, chemical vapor deposition, and ultraviolet ozone treatment.[35−39] For example, Lin and Yang. obtained hierarchical structures by depositing silicon nanoparticles on the wrinkled surface and found that the hierarchical structures not only improved the apparent contact angle but also decreased the contact angle hysteresis.[40] However, the uncontrollable size and morphology of the nanostructures and the use of expensive equipment limited the application of this method. Additionally, when utilizing the mechanical instabilities on the soft surface, some hierarchical structures can also be obtained.[41−45] For

Received: February 28, 2019
Revised: April 29, 2019
Published: May 1, 2019

DOI: 10.1021/acs.langmuir.9b00599
Langmuir 2019, 35, 6870−6877

example, wrinkled structures with various sizes can be prepared from one template by the prestrain to generate well-defined and complex topological features.[46,47]

In practical applications, it is important to tune the wettability of the surface dynamically. A large number of studies show that the wettability of the surface can be controlled by external stimuli such as electric field, temperature, pH, ultraviolet light, and mechanical regulation.[48−52] Compared with temperature, pH, or light control, mechanical regulation is simpler and safer. There is also no special requirement for used materials and preparation processes. Zhao et al. fabricated hierarchically wrinkled surfaces on the polydimethylsiloxane (PDMS) film by photolithography and soft lithography. The increase in the mechanical strain with different directions resulted in the primary anisotropic wetting of the surface becoming isotropic or anisotropic dependent in the contact angle ranges from 120° to 138°.[53] Goel et al. prepared a silver-based wrinkled microstructure on the prestretched PDMS surface using the oblique deposition method, and the apparent contact angle could be reversibly changed from 126.2° to 154.8° (from hydrophobic to superhydrophobic) by adjusting the mechanical strain.[54] Unfortunately, the wetting state of the material surface was of instability during the multiple cycles. Therefore, the prediction of the wetting state of the surface of hierarchical structures and relationship between the contact angle and the strain via the theoretical investigation is necessary, which will be instructive and meaningful to the preparation of hierarchical structures with both a large range of contact angle variation and good repeatability under external strain.

In this study, a thermodynamic approach was used to analyze the wetting states of a droplet on the hierarchically wrinkled surface. We established a theoretical framework to understand how the prestrain and applied dynamic strain reversibly tune the wettability of the hierarchically wrinkled surface. We also experimentally prepared a hierarchically wrinkled surface through a prestretch process and template method with the wettability of the surface dynamically tuned from superhydrophobic to hydrophobic. After multiple stretching and release cycle tests, the experimental results were in agreement with the theoretical prediction. This will provide a theoretical guidance for reversible tuning of surface wettability in a controlled fashion used in microfluidic valves, micro- and nanofabrication of complex structures, and cell transport manipulation.

THEORETICAL BASIS

Wetting States of a Droplet on the Hierarchically Wrinkled Surface. To analyze the wettability of the hierarchically wrinkled surface, as shown in Figure 1a, we establish a model of a droplet on surfaces with a wrinkled pattern and strip structures. We simplify the three-dimensional model to a two-dimensional one and just investigate the contact angle in the plane vertical to the strip direction. First, we analyze the cross section of the wrinkled structures with a droplet on it. Owing to the arc-shape of the top of wrinkled structures, the liquid level of the droplet will not form a tangent to the top of the wrinkled structures but will certainly wet some of the area (Figure 1b). Assume that the shape of the wrinkled structures matches a cosine function; then, the shape function of the solid surface can be expressed as $y = A\cos\left(\frac{2\pi}{\lambda}x\right)$. According to the previous studies,[29,32,40,55]

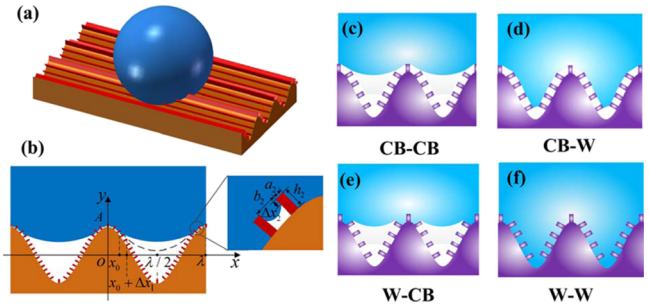

Figure 1. Schematic diagram of droplet infiltration and wetting states of a water droplet on a hierarchically wrinkled surface. (a) 3D schematic diagram of a droplet on the wrinkled surface with strip structures. (b) Schematic diagram of a general water droplet on a hierarchically wrinkled surface. (c−f) Wetting states of a water droplet on a hierarchically wrinkled surface: (c) CB−CB (Cassie−Baxter) state, (d) CB−W (Wenzel) state, (e) W−CB state, and (f) W−W state.

the wavelength λ and amplitude A can be written as $\lambda = 2\pi h_f\left(\frac{\bar{E}_f}{3\bar{E}_s}\right)^{1/3}$ and $A = h_f\left(\frac{\varepsilon}{\varepsilon_c} - 1\right)^{1/2}$. Here, h_f is the film thickness and ε is the applied strain. The subscripts f and s refer to the top film (e.g., PDMS) and bottom substrate (e.g., viscous elastomer film VHB), respectively. In addition, $\bar{E} = E/(1-\nu^2)$ is the plane-strain modulus, E is the Young's modulus, ν is the Poisson's ratio, and $\varepsilon_c = \frac{1}{4}\left(\frac{3\bar{E}_s}{\bar{E}_f}\right)^{2/3}$ is the critical strain applied for the formation of wrinkles.[56,57]

For a droplet on this surface, $x_0\left(0 \le \frac{x_0}{\lambda} \le \frac{1}{2}\right)$ is the liquid contact position, and Δx_1 and Δx_2 represent the infiltration depth of the droplet on the wrinkled structures and strip structures, respectively (Figure 1b). L_{ext} is the length of the outer surface of the droplet at the cross section. The geometrical relation can be obtained with $L_{ext} = 2\theta R$, where R is the radius of the droplet and θ is the contact angle. L_{base} is the length of the contact between the droplet and substrate, and the geometrical relation is $L_{base} = 2R\sin\theta$. L_{total} corresponds to the total length of the substrate.[15] The schematic illustration of L_{ext}, L_{base}, and L_{total} is shown in Figure S1. Assume that S is the area of the droplet cross section, and the relation between the radius R and the contact angle θ is given by $R = \sqrt{\frac{S}{\theta - \sin\theta\cos\theta}}$.

Considering the strip structure of the hierarchically wrinkled surface, we denote the side length of the strip structure as a_2, with spacing b_2 and strip height of h_2. Then, the total free energy of the system G includes the interfacial free energy and potential energy, which can be expressed as[58]

$$G = \gamma_{LV}L_{LV} + \gamma_{SV}L_{SV} + \gamma_{SL}L_{SL} \quad (1)$$

where γ_{LV}, γ_{SV}, and γ_{SL} are the interfacial tension of the liquid−vapor interface, solid−vapor interface and solid−liquid interface, respectively. L_{LV}, L_{SV}, and L_{SL} are the length of the liquid−vapor interface, solid−vapor interface, and solid−liquid interface, respectively.

Equation of Contact Angle. For a droplet on a rough surface, it is either in a Wenzel (W) state or in a CB state.[59,60] Taking into account the different positions of the triple contact point x_0, Δx_1, and Δx_2 in this model, the droplets will be in different wetting states. In our previous study,[10,11] a

DOI: 10.1021/acs.langmuir.9b00599
Langmuir 2019, 35, 6870−6877

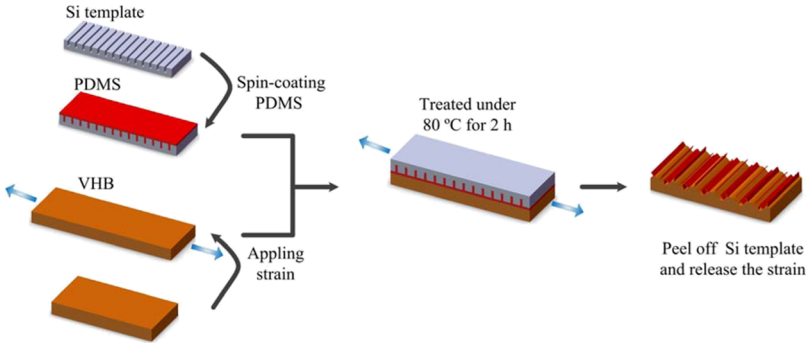

Figure 2. Schematic description of preparation of hierarchically wrinkled surface by the relaxation of PDMS film with strip structures on the prestretched VHB film.

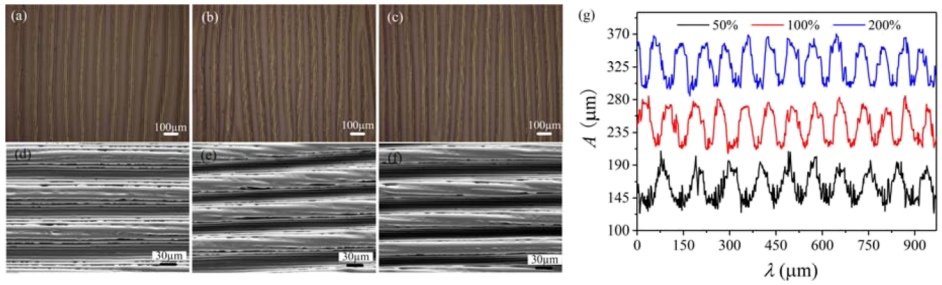

Figure 3. Characterization of the hierarchically wrinkled surfaces with different amounts of prestrain. (a–c) Laser microscopy images of the hierarchically wrinkled surfaces with different amounts of prestrain: (a) ε_{pre} = 50%, (b) ε_{pre} = 100%, (c) ε_{pre} = 200%. (d–f) High magnified SEM images of the hierarchically wrinkled surfaces with different amounts of prestrain: (d) ε_{pre} = 50%, (e) ε_{pre} = 100%, (f) ε_{pre} = 200%. The width and height of strip structures are 10 and 10 μm, respectively. (g) Numerical results from laser microscope of hierarchically wrinkled surfaces with different amounts of prestrain. The black, red, and blue lines represent the amount of prestrain of 50, 100, and 200%, respectively. The relative wrinkled height of the samples is A/λ = 0.247 = 0.025, A/λ = 0.35 5 0.02, and A/λ = 0.435 00.035, respectively.

thermodynamic approach was used to analyze all wetting states of a water droplet on dual-scale rough surfaces with structured sidewalls. This method is also suitable here. Detailed derivation is described in Part S1 of the Supporting Information.

According to the principle of minimum free energy[61] and eq 1, the wetting states include four stable states, namely, CB–CB, CB–W, W–CB, and W–W states, as shown in Figure 1c–f. The front symbol represents the wetting state of strip structure, and the back one represents the wetting state of wrinkled structure. The contact angle equation of the four wetting states can be expressed as follows

$$\cos\theta_{CB-CB} = r_f f_1 f_2 \cos\theta_0 + r_f f_1 f_2 - r_f f_1 + f_1 - 1 \quad (2)$$

$$\cos\theta_{CB-W} = r_1 f_2 \cos\theta_0 + r_1 f_2 - r_1 \quad (3)$$

$$\cos\theta_{W-CB} = r_f r_2 f_1 \cos\theta_0 + f_1 - 1 \quad (4)$$

$$\cos\theta_{W-W} = r_1 r_2 \cos\theta_0 \quad (5)$$

Here, f is the length fraction that can be given by $f_1 = \frac{2x_0}{\lambda}$, $f_2 = \frac{a_2}{a_2 + b_2}$, r is the rough factor that is given by $r_1 = \frac{\int_{-\lambda/2}^{\lambda/2} \sqrt{1 + y'^2}\, dx}{\lambda}$, $r_2 = \frac{a_2 + b_2 + 2h_2}{a_2 + b_2}$, $r_f = \frac{\int_{-x_0}^{x_0} \sqrt{1 + y'^2}\, dx}{2x_0}$. θ_0 is the intrinsic contact angle and y' is the derivative of y $\left(y = A\cos\left(\frac{2\pi}{\lambda}x\right)\right)$. Furthermore, because of the flexibility of the substrate, the prestretch ε can affect the relative height (A/λ) so that the θ is also altered. Because of these unique features, precise control of the θ with the wrinkled surface becomes possible.[62]

$$\frac{A}{\lambda} = \frac{1}{\pi}\sqrt{\varepsilon - \varepsilon_c} \quad (6)$$

By substituting eq 6 into the θ in different wetting states, the relationship between the prestrain ε and θ can be obtained.

EXPERIMENTAL SECTION

Preparation of the PDMS Solution. The PDMS solution was prepared by mixing a prepolymer (Sylgard 184, Dow Corning) with a curing agent in a 10:1 ratio at room temperature and degassed in a vacuum oven for 30 min to remove all bubbles from the viscous liquid.

Preparation of Hierarchically Wrinkled Substrates. The fabrication process for the hierarchically wrinkled surface is shown in Figure 2. The commercial Si templates with strip structures were fabricated by the wet etching technique. The width and height of strip structures were 10 and 10 μm, respectively, and the strip spacing was 3, 5, 10, and 20 μm, respectively. After immersion in "piranha" etch solution (70% H_2SO_4, 30% H_2O_2, 90 °C), the patterned Si template was cleaned with deionized water and then immersed into a solution consisting of 10 mL of *n*-heptane, 0.2 mL of trimethoxyoctadecylsilane, and 0.5 mL of ethyl acetate for 2 h for hydrophobic treatment. Then, the Si template was annealed in an oven at 100 °C for 1 h. The well-prepared PDMS solution was spun-coated on the Si template at 8000 rpm for 20 s. The thickness of the PDMS film was controlled about 150 μm. Next, the Si template with covered PDMS was placed into the oven and cured for 8 min at 80 °C. After the PDMS side was adhered onto a prestrained viscous elastomer film (VHB 4910, 3 M Inc., US) by a clamp device (Figure S2a, the amount of prestrain was easy controlled by the clamp device), they were put into the oven together and cured for 2 h at 80 °C. During this process, the strain was kept by the clamp device. After cooling and peeling off the Si template, the patterned PDMS film was transferred onto the prestrained VHB film. Finally, the strain was slowly released and

DOI: 10.1021/acs.langmuir.9b00599
Langmuir 2019, 35, 6870–6877

the wrinkled structures with the strip structures were formed from the internal buckling of the PDMS elastomer film. The wrinkled PDMS films without the strip structures were also prepared for control experiments.

Characterization. The morphologies of the hierarchically wrinkled surfaces with different amounts of prestrain were analyzed by a laser microscope (Keyence, VK-X100, Figure 3a–c) and scanning electron microscopy (SEM, Hitachi S4800, Figure 3d–f). The droplet contact angle (θ) was measured using 4 μL of droplets of deionized water with a contact angle instrument (Thermo, DCA-322). The water drops were dispensed using a syringe pump through a needle with 100 μm inner diameter. It can be seen from Figure 3a–f that as the amount of prestrain increases, the wavelength (λ) of the structure decreases. Numerical results from a laser microscope (Figure 3g) show that the relative height (A/λ) of the wrinkled structures gradually increases with increasing amount of prestretching. Comparing the numerical results of the wrinkled structures with and without the strip structures under the same amount of prestrain (Figure S3-1), it can be seen that the strip structure has a little effect on the size of the wrinkled structure. The morphologies of the strip structures and their respective θ are shown in Figure S3-2a–d. The morphologies of the hierarchically wrinkled surfaces and their respective θ are shown in Figure S3-2e–h. We find that as the spacing increases, the change in θ shows a tendency to increase first and then decrease.

RESULTS AND DISCUSSION

Lotus leaves have excellent superhydrophobicity, largely because of the droplets on the surface being in a CB state with a big contact angle.[8,9] Therefore, it is of great importance to the stability of superhydrophobic surfaces that the droplet remains in a CB–CB state as much as possible. This should be possible by controlling the size of the wrinkle and strip structures. To further analyze the influence of the size of the structures on the wetting states of the droplets, we assign $0 \le b_2/a_2 \le 1$, $0 \le A/\lambda \le 1$ and an intrinsic contact angle $\theta_0 = 120°$. Figure 4 shows the wetting phase diagram of four stable wetting states of the droplet which can be divided into four regions. When $A/\lambda \le 0.3$, the θ is much lower than that in the case of $0.3 \le A/\lambda \le 1$. In the following section, the relationship between the size of each structure and θ will be discussed.

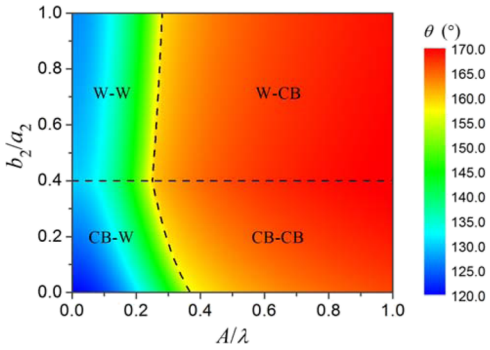

Figure 4. Wetting phase diagram of four stable wetting states. The apparent contact angle (θ) of a water droplet on the surface in four stable wetting states, as a function of the relative spacing of wrinkled strip structures.

As shown in Figure 5a, taking $A/\lambda = 0.3$, changing the spacing between strips (b_2) at a fixed width (a_2), and when $0 \le b_2/a_2 \le 0.18$, the droplets are in a CB–W state. From a thermodynamic point of view, the droplets tend to wet the wrinkled structures. The droplets then attain a CB–CB state when $0.18 \le b_2/a_2 \le 0.4$, and the θ reaches a peak (163°) with the increase of b_2/a_2. However, as the spacing of the strip structures continues to increase ($0.4 \le b_2/a_2 \le 1.65$), θ begins to decrease from 164° to 159°. At this point, the droplets exist in a W–CB state. Similarly, θ still decreases with the increasing spacing of the strip structures when the droplets exist in a W–W state. In addition, the wetting state of the strip surface changes from CB to W following an increase in the size of the strip. The wetting state of the wrinkled structure changes from W to CB first and then from CB to W. This shows that the change in the size of the strip structures will affect the wetting states of the wrinkled structures, and as the b_2/a_2 increases, the contact angle increases first and then decreases. Besides, the effect of the strip height on wetting states is shown in Figure S4. It can be seen that as the h_2/a_2 increases, the range of b_2/a_2 in which the droplets are in the CB–CB state becomes larger.

Likewise, if the size of the strip remains unchanged, the change in the size of the wrinkled structures will also affect the wetting state of the droplets, as shown in Figure 5b. Following a change in the strip's size, the analysis result from a thermodynamic point of view shows that the wetting states of the droplets can be divided into two regions. When $b_2/a_2 = 0.5$ and $A/\lambda = 0.26$, the droplets are in a W–W state, indicating that the strip and wrinkled structure are both wetted. When $A/\lambda \ge 0.26$, the droplets are in a W–CB state, indicating that the strip structures are being wetted but the wrinkled structures are not being immersed. Following a change in the size of the strip structure, it is possible to find "point-of-variability". At the left of the point, θ of the droplet increases sharply and the wrinkled structure is in a Wenzel state. Conversely, it can be found that the wetting state of the strip structures does not change with a change in the size of the wrinkled structures. The transition of the wetting state involves the change of the energy barrier. The detailed analysis of the energy barrier is shown in Part S5 in the Supporting Information. Our results indicate that the wrinkled structure and strip structures increase the stability of the structure. On the other hand, under the same deformation, different sized strip structures show different contact angle ranges. Therefore, strip structures of an appropriate size are conducive to broadening the tunable range of the θ.

Influence of the Intrinsic Contact Angle and Elastic Modulus on the Wetting States. As discussed above, the sizes of the strip structures and wrinkled structures affect the wettability of the surface. The structure of the strips can be controlled by soft lithography. However, the relationship between the size of the wrinkled structure and prestretch must be determined. We chose the VHB and PDMS system for investigation. According to the different Young's modulus between a film and a substrate, compared with theory[63] (Figure S6), the size of the wrinkled structures can be found to be in good agreement with the theoretical values and within the allowed range of error. Following an increase in the ratio of the elastic modulus E_s/E_f, a wrinkled pattern is more difficult to form, but the size of the wrinkled structure A/λ increases as a result of the increasing prestretch. Moreover, the ratio of the elastic modulus E_s/E_f of the selected materials (VHB and PDMS) is approximately 5×10^{-4}, and further increasing this ratio does not alter the theoretical prediction. Besides, because of the high adhesion of VHB and flexibility of PDMS, there is no delamination between materials under strain during the experiment. These suggest that the two materials, VHB and PDMS, are suitable for the fabrication of wrinkled structures.

DOI: 10.1021/acs.langmuir.9b00599
Langmuir 2019, 35, 6870–6877

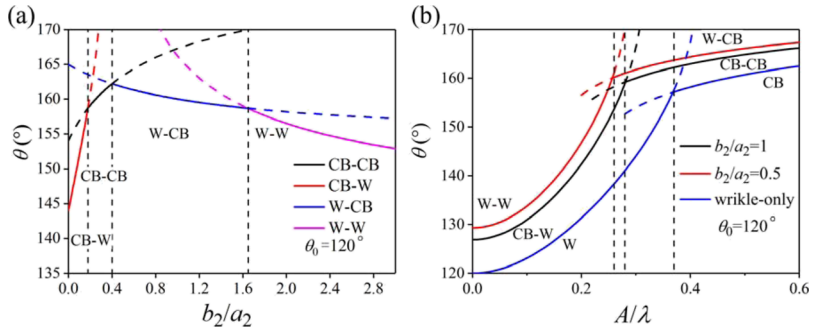

Figure 5. (a) Relationship between the size of strip b_2/a_2 and apparent contact angle θ with A/λ = 0.3. (b) Relationship between the apparent contact angle θ and the size of the wrinkled structure A/λ at different strip structures (b_2/a_2).

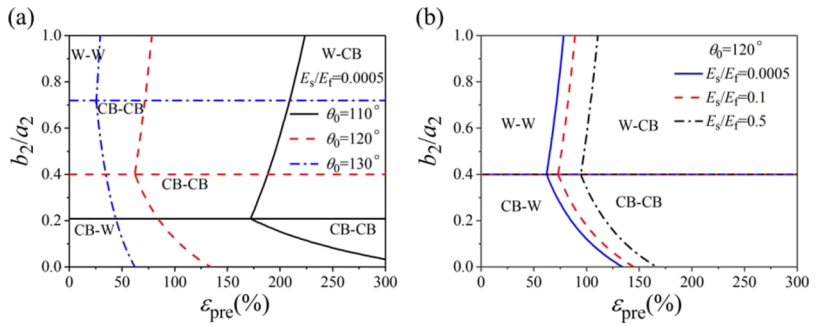

Figure 6. Phase diagram depicting the influence of (a) intrinsic contact angle θ_0 and (b) elastic modulus of the substrate on the wetting state. The amount of prestrain ε_{pre} can be converted to A/λ using Figure S6.

Not only does the elastic modulus of the substrate affect the wettability of the hierarchically wrinkled surface but also the intrinsic contact angle θ_0 also influences it. Figure 6 shows the impact of the θ_0 and the ratio of the elastic modulus of the substrates on the CB−CB state. Following an increase in the θ_0 (Figure 6a), the region corresponding to the CB−CB state also increases, indicating that it is beneficial to maintaining a CB−CB state of the droplet on the surface. The CB−CB area gradually increases following a decrease in the ratio of the elastic modulus E_s/E_f (Figure 6b), indicating that the film becomes harder or the substrate becomes softer; these phenomena are both conducive to maintaining a CB−CB state. The prestretch ε_{pre} in Figure 6 can be converted to A/λ using Figure S6. Superhydrophobic surfaces can therefore be reasonably designed via the selection of the intrinsic contact angle and elastic modulus of the substrate.

Influence of Prestretch on the Wettability of the Hierarchically Wrinkled Surface. The wetting of a water drop on the hierarchically wrinkled surface was investigated at different amounts of prestretch and dynamic strain. Pictures of stretching and unloading in a real system are shown in Figure S2b−d. Figure 7 shows the experimentally observed and theoretically determined θ of the hierarchically wrinkled surface for different amounts of prestrain when θ_0 = 120°. Control experiments were conducted on the wrinkled surfaces without a strip structure. During a gradual increase in prestretching, the wetting state of the droplet on the hierarchically wrinkled surface changes from the W−W state to W−CB one, and the θ changes from 126° to nearly 165° in terms of theory. The increase in hydrophobicity is caused by the enhancement of the relative height of the wrinkled structure; the strip structures are wetted while the wrinkled structures are in the CB state following prestretching. Within the limit of allowable errors, our contact angle equations

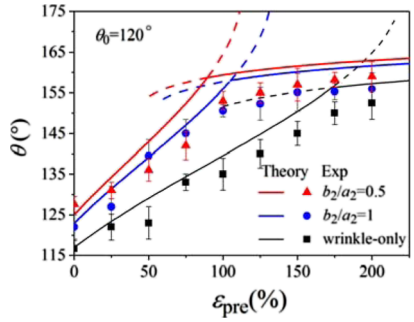

Figure 7. Relationship between the apparent contact angle θ and the amount of prestretch ε_{pre}. In terms of theory, θ increases from 124° to 165° with the increasing amount of prestretch. The spot on the graph is the experimental value, with the intrinsic contact angle θ_0 = 120° of the substrate.

shown in eqs 2−5 are in good agreement with experimentally observed values. This demonstrates that the superhydrophobicity can be achieved using a hierarchically wrinkled surface and that the θ is tunable by controlling the prestretch.

Influence of Applied Stretching on the Wettability of the Hierarchically Wrinkled Surface. Another advantage of this hierarchically wrinkled surface is that dynamic strain can be applied so that the θ can be adjusted accordingly. At the amount of prestretch of 200%, stable repulsive superhydrophobicity is achieved, resulting in a static contact angle in excess of 150° (Figure 8a). As the amount of dynamic strain increases, the θ decreases in line with a decrease in the relative height of the wrinkled structures. When the amount of dynamic strain is lower than a threshold value, the droplets on the hierarchically wrinkled surface are in a W−CB state. As the dynamic strain is applied, the droplets preferentially wet the

DOI: 10.1021/acs.langmuir.9b00599
Langmuir 2019, 35, 6870−6877

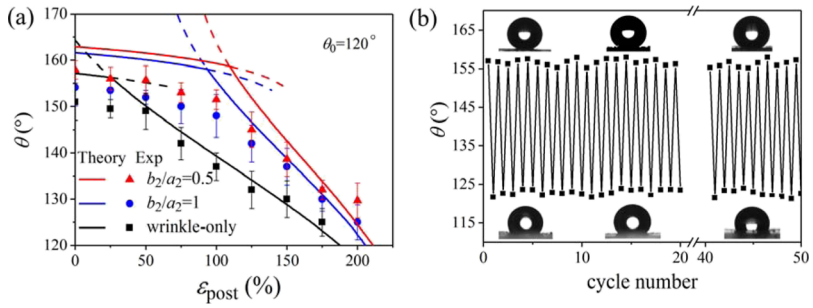

Figure 8. (a) Relationship between the apparent contact angle θ and amount of dynamic strain ε_{post}. The spot on the graph is the experimental value, with the intrinsic contact angle of the substrate θ_0 = 120°. θ decreases from 157° to 124° as ε_{post} increases. (b) Fully reversible cyclic switching of θ by applying a dynamic strain of 200% and relaxation. The substrate was prestretched at 200%, and the θ changes from approximately 157° to 123°.

wrinkled pattern so that the wetting states change from W−CB to W−W.

Because of the excellent elastic recovery of the VHB substrate, multiple stretching and releasing cycles were applied. Cyclic dynamic switching was conducted at 200% prestretching of the substrate by periodic application of 200% dynamic strain and relaxation. First, the soft substrate was gradually stretched to three times as long as its original length, and then, the dynamic strain was released. θ is consistently tuned from 157° to 123° between each cycle, namely, from superhydrophobic to hydrophobic. As can be seen from Figure 8b, even if the stretching−releasing cycle was applied repeatedly over 50 cycles, the surface retains the wettability. This suggests that the wetting switch is reversible and that the hierarchically wrinkled surface is tunable and stable.

CONCLUSIONS

In conclusion, a theoretical framework was established to understand how the prestrain and applied dynamic strain reversibly tunes the wettability of a hierarchically wrinkled surface. Specifically, we first established the relationship between the contact angle and structural size using a thermodynamic equation, which included the wrinkling structure size and strip structure size; we then established the relationship between strain and wrinkled structure size and the relationship between strain and contact angle. Through theoretical analysis and related experiments, we have shown that the wettability of the surface can be controlled by applying different amounts of prestretch and external strain, which can mostly be attributed to the change in structural the size and energy barrier. Furthermore, the surface wettability can be adjusted from superhydrophobic to hydrophobic, even after multiple stretching-release cycles. This research may provide insights into the design of soft surfaces for tunable wetting and motivate further research for mechanically tunable surfaces.

ASSOCIATED CONTENT

Supporting Information

The Supporting Information is available free of charge on the ACS Publications website at DOI: 10.1021/acs.langmuir.9b00599.

Thermodynamic analysis of wetting states on the hierarchically wrinkled surface, experimental setup, laser micrograph of the wrinkled structures and hierarchically wrinkled structures under the same amount of prestrain, morphology of the strip structures and the hierarchically wrinkled surfaces and their respective apparent contact angle, effect of strip height on wetting states, analysis of the energy barrier in the wetting transition, and relationship between prestretching and the size of the wrinkled structure (PDF)

AUTHOR INFORMATION

Corresponding Authors

*E-mail: wuhuaping@gmail.com (H.W.).
*E-mail: chaigz@zjut.edu.cn (G.C.).

ORCID

Huaping Wu: 0000-0003-4505-7062

Notes

The authors declare no competing financial interest.

ACKNOWLEDGMENTS

This work was supported by the National Science Foundation of China (grant nos. 11372280, 11672269, and 51675485), the Zhejiang Provincial Natural Science Foundation of China (grant nos. LR19E020004 and LR18E050002).

REFERENCES

(1) Khojasteh, D.; Kazerooni, M.; Salarian, S.; Kamali, R. Droplet impact on superhydrophobic surfaces: A review of recent developments. *J. Ind. Eng. Chem.* **2016**, *42*, 1−14.
(2) Wang, X.; Liu, A.; Xing, Y.; Duan, H.; Xu, W.; Zhou, Q.; Wu, H.; Chen, C.; Chen, B. Three-Dimensional Graphene Biointerface with Extremely High Sensitivity to Single Cancer Cell Monitoring. *Biosens. Bioelectron.* **2018**, *105*, 22−28.
(3) Simpson, J. T.; Hunter, S. R.; Aytug, T. Superhydrophobic Materials and Coatings: a Review. *Rep. Prog. Phys.* **2015**, *78*, 086501.
(4) Kong, X.; Zhang, J.; Xuan, Q.; Lu, J.; Feng, J. Superhydrophobic Coating for Anti-fouling of Chinese Paintings. *Langmuir* **2018**, *34*, 8294−8301.
(5) Zhang, J.; Lin, W.; Zhu, C.; Lv, J.; Zhang, W.; Feng, J. Dark, Infrared Reflective, and Superhydrophobic Coatings by Waterborne Resins. *Langmuir* **2018**, *34*, 5600−5605.
(6) Wu, H.; Zhu, K.; Cao, B.; Zhang, Z.; Wu, B.; Liang, L.; Chai, G. Smart Design of Wettability-Patterned Gradients on Substrate-Independent Coated Surfaces to Control Unidirectional Spreading of Droplets. *Soft Matter* **2017**, *13*, 2995−3002.
(7) Qiu, X.; Yang, Z.; Wu, H.; Guo, J.; Zhang, Z.; Feng, J.; Chai, G. Excellent Oil-Water Separation under External Pressure: Controllable Critical Pressure and Separation Efficiency by Well-Designed Hierarchical Mesh Structure. *Appl. Surf. Sci.* **2018**, *456*, 602−608.
(8) Barthlott, W.; Neinhuis, C. Purity of the Sacred Lotus, or Escape from Contamination in Biological Surfaces. *Planta* **1997**, *202*, 1−8.
(9) Neinhuis, C.; Barthlott, W. Characterization and Distribution of Water-Repellent, Self-Cleaning Plant Surfaces. *Ann. Bot.* **1997**, *79*, 667−677.

DOI: 10.1021/acs.langmuir.9b00599
Langmuir 2019, 35, 6870−6877

(10) Wu, H.; Zhu, K.; Wu, B.; Lou, J.; Zhang, Z.; Chai, G. Influence of Structured Sidewalls on the Wetting States and Superhydrophobic Stability of Surfaces with Dual-Scale Roughness. *Appl. Surf. Sci.* **2016**, *382*, 111−120.
(11) Wu, H.; Yang, Z.; Cao, B.; Zhang, Z.; Zhu, K.; Wu, B.; Jiang, S.; Chai, G. Wetting and Dewetting Transitions on Submerged Superhydrophobic Surfaces with Hierarchical Structures. *Langmuir* **2017**, *33*, 407−416.
(12) Park, H. K.; Yoon, S. W.; Do, Y. R. Superhydrophobicity of 2D SiO2 Hierarchical Micro/Nanorod Structures Fabricated Using a Two-Step Micro/Nanosphere Lithography. *J. Mater. Chem.* **2012**, *22*, 14035−14041.
(13) Feng, J.; Tuominen, M. T.; Rothstein, J. P. Hierarchical Superhydrophobic Surfaces Fabricated by Dual-Scale Electron-Beam-Lithography with Well-Ordered Secondary Nanostructures. *Adv. Funct. Mater.* **2011**, *21*, 3715−3722.
(14) Guo, Z.; Zhou, F.; Hao, J.; Liu, W. Stable Biomimetic Superhydrophobic Engineering Materials. *J. Am. Chem. Soc.* **2005**, *127*, 15670−15671.
(15) Cha, T.-G.; Yi, J. W.; Moon, M.-W.; Lee, K.-R.; Kim, H.-Y. Nanoscale Patterning of Microtextured Surfaces to Control Superhydrophobic Robustness. *Langmuir* **2010**, *26*, 8319−8326.
(16) Wang, Z.; Chen, E.; Zhao, Y. The Effect of Surface Anisotropy on Contact Angles and the Characterization of Elliptical Cap Droplets. *Sci. China: Technol. Sci.* **2018**, *61*, 309−316.
(17) Zhao, Y.-P.; Yuan, Q. Statics and Dynamics of Electrowetting on Pillar-Arrayed Surfaces at the Nanoscale. *Nanoscale* **2015**, *7*, 2561−2567.
(18) Yuan, Q.; Zhao, Y.-P. Multiscale dynamic wetting of a droplet on a lyophilic pillar-arrayed surface. *J. Fluid Mech.* **2013**, *716*, 171−188.
(19) Hamley, I. W. Nanotechnology with Soft Materials. *Angew. Chem., Int. Ed.* **2003**, *42*, 1692−1712.
(20) Quake, S. R.; Scherer, A. From Micro-to Nanofabrication with Soft Materials. *Science* **2000**, *290*, 1536−1540.
(21) Tan, D P.; Zhang, L. P.; Ai, Q. L. An Embedded Self-Adapting Network Service Framework for Networked Manufacturing System. *Intell. Manuf.* **2019**, *30*, 539−556.
(22) Tan, D. P.; Li, L.; Zhu, Y. L.; Zheng, S.; Yin, Z. C.; Li, D. F. Critical Penetration Condition and Ekman Suction-Extraction Mechanism of a Sink Vortex. *J. Zhejiang Univ., Sci., A* **2019**, *20*, 61−72.
(23) Sekine, J.; Luo, S.-C.; Wang, S.; Zhu, B.; Tseng, H.-R.; Yu, H.-h. Functionalized Conducting Polymer Nanodots for Enhanced Cell Capturing: The Synergistic Effect of Capture Agents and Nanostructures. *Adv. Mater.* **2011**, *23*, 4788−4792.
(24) Cui, Y.; Li, Y.; Xing, Y. Sweat Effects on The Thermal Analysis of Epidermal Electronic Devices Integrated with Human Skin. *Int. J. Heat Mass Transfer* **2018**, *127*, 97−104.
(25) Persano, L.; Dagdeviren, C.; Su, Y. W.; Zhang, Y. H.; Girardo, S.; Pisignano, D.; Huang, Y. G.; Rogers, J. A. High Performance Piezoelectric Devices Based on Aligned Arrays of Nanofibers of Poly(vinylidenefluoride-co-trifluoroethylene). *Nat. Commun.* **2013**, *4*, 1633.
(26) Dagdeviren, C.; Su, Y. W.; Joe, P.; Yona, R.; Liu, Y. H.; Kim, Y. S.; Huang, Y. A.; Damadoran, A. R.; Xia, J.; Martin, L. W. Conformable Amplified Lead Zirconate Titanate Sensors With Enhanced Piezoelectric Response for Cutaneous Pressure Monitoring. *Nat. Commun.* **2014**, *5*, 4496.
(27) Li, L.; Bai, Y.; Li, L.; Wang, S.; Zhang, T. A Superhydrophobic Smart Coating for Flexible and Wearable Sensing Electronics. *Adv. Mater.* **2017**, *29*, 1702517.
(28) Prathapan, R.; Berry, J. D.; Garnier, G.; Tabor, R. F.; Tabor, R. F. Decreasing the Wettability of Cellulose Nanocrystal Surfaces Using Wrinkle-Based Alignment. *ACS Appl. Mater. Interfaces* **2017**, *9*, 15202−15211.
(29) Lee, J.-H.; Ro, H. W.; Huang, R.; Lemaillet, P.; Germer, T. A.; Soles, C. L.; Stafford, C. M. Anisotropic, Hierarchical Surface Patterns via Surface Wrinkling of Nanopatterned Polymer Films. *Nano Lett.* **2012**, *12*, 5995−5999.
(30) Roy, P. K.; Pant, R.; Nagarajan, A. K.; Khare, K. Mechanically Tunable Slippery Behavior on Soft Poly(dimethylsiloxane)-Based Anisotropic Wrinkles Infused with Lubricating Fluid. *Langmuir* **2016**, *32*, 5738−5743.
(31) Saha, S. K.; Culpepper, M. L. Deterministic Switching of Hierarchy during Wrinkling in Quasi-Planar Bilayers. *Adv. Eng. Mater.* **2016**, *18*, 938−943.
(32) Liu, J.-L.; Feng, X.-Q.; Wang, G.; Yu, S.-W. Mechanisms of Superhydrophobicity on Hydrophilic Substrates. *J. Phys.: Condens. Matter* **2007**, *19*, 356002.
(33) Yang, S.; Khare, K.; Lin, P.-C. Harnessing Surface Wrinkle Patterns in Soft Matter. *Adv. Funct. Mater.* **2010**, *20*, 2550.
(34) Zhang, Z.; Zhang, T.; Zhang, Y. W.; Kim, K.-S.; Gao, H. Strain-Controlled Switching of Hierarchically Wrinkled Surfaces Between Superhydrophobicity and Superhydrophilicity. *Langmuir* **2012**, *28*, 2753−2760.
(35) Xia, Y.; Whitesides, G. M. Soft Lithography. *Angew. Chem., Int. Ed.* **1998**, *37*, 550−575.
(36) Qin, D.; Xia, Y.; Whitesides, G. M. Soft Lithography for Micro- and Nanoscale Patterning. *Nat. Protoc.* **2010**, *5*, 491−502.
(37) Barkusky, F.; Peth, C.; Bayer, A.; Mann, K. Direct Photo-Etching of Poly (Methyl methacrylate) Using Focused Extreme Ultraviolet Radiation From a Table-Top Laser-Induced Plasma Source. *J. Appl. Phys.* **2017**, *101*, 124908.
(38) Coclite, A. M.; Howden, R. M.; Borrelli, D. C.; Petruczok, C. D.; Yang, R.; Yagüe, J. L.; Ugur, A.; Chen, N.; Lee, S.; Jo, W. J.; Liu, X.; Gleason, K. K. 25th Anniversary Article: CVD Polymers: A New Paradigm for Surface Modifi cation and Device Fabrication. *Adv. Mater.* **2013**, *25*, 5392−5423.
(39) Childs, W. R.; Motala, M. J.; Lee, K. J.; Nuzzo, R. G. Masterless Soft Lithography: Patterning UV/Ozone-Induced Adhesion on Poly(dimethylsiloxane) Surfaces. *Langmuir* **2005**, *21*, 10096−10105.
(40) Lin, P.-C.; Yang, S. Mechanically Switchable Wetting on Wrinkled Elastomers with Dual-Scale Roughness. *Soft Mater.* **2009**, *5*, 1011−1018.
(41) Das, A.; Banerji, A.; Mukherjee, R. Programming Feature Size in the Thermal Wrinkling of Metal Polymer Bilayer by Modulating Substrate Viscoelasticity. *ACS Appl. Mater. Interfaces* **2017**, *9*, 23255−23262.
(42) Bhandaru, N.; Goohpattader, P. S.; Faruqui, D.; Mukherjee, R.; Sharma, A. Solvent Vapor Assisted Dewetting of Pre-Patterned Thin Polymer Films: Control of Morphology, Order and Pattern Miniaturization. *Langmuir* **2015**, *31*, 3203−3214.
(43) Yoo, P. J.; Suh, K. Y.; Park, S. Y.; Lee, H. H. Physical Self-Assembly of Microstructures by Anisotropic Buckling. *Adv. Mater.* **2002**, *14*, 1383−1387.
(44) Yang, X.; Zhao, Y.; Xie, J.; Han, X.; Wang, J.; Zong, C.; Ji, H.; Zhao, J.; Jiang, S.; Cao, Y.; Lu, C. Bioinspired Fabrication of Free-Standing Conducting Films with Hierarchical Surface Wrinkling Patterns. *ACS Nano* **2016**, *10*, 3801−3808.
(45) Chen, C.-M.; Yang, S. Wrinkling Instabilities in Polymer Films and Their Applications. *Polym. Int.* **2012**, *61*, 1041−1047.
(46) Zang, J.; Ryu, S.; Pugno, N.; Wang, Q.; Tu, Q.; Buehler, M. J.; Zhao, X. Multifunctionality and Control of the Crumpling and Unfolding of Large-Area Graphene. *Nat. Mater.* **2013**, *12*, 321−325.
(47) Zeng, S.; Li, R.; Freire, S. G.; Garbellotto, V. M. M.; Huang, E. Y.; Smith, A. T.; Hu, C.; Tait, W. R. T.; Bian, Z.; Zheng, G.; Zhang, D.; Sun, L. Moisture-Responsive Wrinkling Surfaces with Tunable Dynamics. *Adv. Mater.* **2017**, *29*, 1700828.
(48) Kim, T.; Lu, W. Y.; Lim, H.; Han, A. J.; Qiao, Y. Electrically Controlled Hydrophobicity in a Surface Modified Nanoporous Carbon. *Appl. Phys. Lett.* **2011**, *98*, 053106.
(49) He, M.; Li, H.; Wang, J. J.; Song, Y. L. Superhydrophobic Surface at Low Surface Temperature. *Appl. Phys. Lett.* **2011**, *98*, 093118.
(50) Stratakis, E.; Mateescu, A.; Barberoglou, M.; Vamvakaki, M.; Fotakis, C.; Anastasiadis, S. H. From Superhydrophobicity and Water

DOI: 10.1021/acs.langmuir.9b00599
Langmuir 2019, 35, 6870−6877

Repellency to Superhydrophilicity: Smart Polymer-Functionalized Surfaces. *Chem. Commun.* **2010**, *46*, 4136−4138.
(51) Cui, H.; Yang, G. Z.; Sun, Y.; Wang, C. X. Reversible Ultraviolet Light-Manipulated Superhydrophobic-to-Superhydrophilic Transition on a Tubular SiC Nanostructure Film. *Appl. Phys. Lett.* **2010**, *97*, 183112.
(52) Wong, W. S. Y.; Gutruf, P.; Sriram, S.; Bhaskaran, M.; Wang, Z.; Tricoli, A. Strain Engineering of Wave-like Nanofibers for Dynamically Switchable Adhesive/Repulsive Surfaces. *Adv. Funct. Mater.* **2016**, *26*, 399−407.
(53) Zhao, S.; Xia, H.; Wu, D.; Lv, C.; Chen, Q.-D.; Ariga, K.; Liu, L.-Q.; Sun, H.-B. Mechanical Stretch for Tunable Wetting From Topological PDMS Film. *Soft Matter* **2013**, *9*, 4236−4240.
(54) Goel, P.; Kumar, S.; Sarkar, J.; Singh, J. P. Mechanical Strain Induced Tunable Anisotropic Wetting on Buckled PDMS Silver Nanorods Arrays. *ACS Appl. Mater. Interfaces* **2015**, *7*, 8419−8426.
(55) Mumm, F.; van Helvoort, A. T. J.; Sikorski, P. Easy Route to Superhydrophobic Copper-Based Wire-Guided Droplet Microfluidic Systems. *ACS Nano* **2009**, *3*, 2647−2652.
(56) Chung, J. Y.; Nolte, A. J.; Stafford, C. M. Surface Wrinkling: a Versatile Platform for Measuring Thin-Film Properties. *Adv. Mater.* **2011**, *23*, 349−368.
(57) Huang, Z. Y.; Hong, W.; Suo, Z. Nonlinear Analyses of Wrinkles in a Film Bonded to a Compliant Substrate. *J. Mech. Phys. Solids* **2005**, *53*, 2101−2118.
(58) Barbieri, L.; Wagner, E.; Hoffmann, P. Water Wetting Transition Parameters of Perfluorinated Substrates With Periodically Distributed Flat-Top Microscale Obstacles. *Langmuir* **2007**, *23*, 1723−1734.
(59) Wenzel, R. N. Resistance of Solid Surfaces to Wetting by Water. *Ind. Eng. Chem.* **1936**, *28*, 988−994.
(60) Cassie, A. B. D.; Baxter, S. Wettability of Porous Surfaces. *Trans. Faraday Soc.* **1944**, *40*, 546−551.
(61) Tuteja, A.; Choi, W.; Ma, M.; Mabry, J. M.; Mazzella, S. A.; Rutledge, G. C.; McKinley, G. H.; Cohen, R. E. Designing Superoleophobic Surfaces. *Science* **2007**, *318*, 1618−1622.
(62) Lin, G.; Chandrasekaran, P.; Lv, C.; Zhang, Q.; Tang, Y.; Han, L.; Yin, J. Self-Similar Hierarchical Wrinkles as a Potential Multifunctional Smart Window with Simultaneously Tunable Transparency, Structural Color, and Droplet Transport. *ACS Appl. Mater. Interfaces* **2017**, *9*, 26510−26517.
(63) Cao, C.; Chan, H. F.; Zang, J.; Leong, K. W.; Zhao, X. Harnessing Localized Ridges for High-Aspect-Ratio Hierarchical Patterns with Dynamic Tunability and Multifunctionality. *Adv. Mater.* **2014**, *26*, 1763−1770.

DOI: 10.1021/acs.langmuir.9b00599
Langmuir 2019, 35, 6870−6877